

# Quantitative analysis of myocardial glucose utilization in patients with left ventricular dysfunction by means of $^{18}\text{F}$ -FDG dynamic positron tomography and three-compartment analysis

Koichi Morita<sup>1</sup>, Chietsugu Katoh<sup>2</sup>, Keiichiro Yoshinaga<sup>1</sup>, Kazuyuki Noriyasu<sup>3</sup>, Megumi Mabuchi<sup>1</sup>, Takahiro Tsukamoto<sup>3</sup>, Hiroyuki Kageyama<sup>1</sup>, Tohru Shiga<sup>1</sup>, Yuji Kuge<sup>2</sup>, Nagara Tamaki<sup>1</sup>

<sup>1</sup> Department of Nuclear Medicine, Hokkaido University Graduate School of Medicine, Kita-15, Nishi-7, Kita-ku, Sapporo 060-8638, Japan

<sup>2</sup> Department of Tracer Kinetics, Hokkaido University Graduate School of Medicine, Kita-ku, Sapporo, Japan

<sup>3</sup> Department of Cardiovascular Medicine, Hokkaido University Graduate School of Medicine, Kita-Ku, Sapporo, Japan

Received: 13 July 2004 / Accepted: 2 December 2004 / Published online: 18 March 2005

© Springer-Verlag 2005

**Abstract.** *Purpose:* Myocardial glucose utilization (MGU) is altered in various heart diseases. The aim of this study was to quantitatively assess regional myocardial glucose utilization in patients with left ventricular (LV) dysfunction by dynamic  $^{18}\text{F}$ -fluorodeoxyglucose positron emission tomography (FDG PET).

*Methods:* A total of 18 subjects were studied, including ten with LV dysfunction (seven with idiopathic dilated cardiomyopathy and three with aortic regurgitation; NYHA II in 8 and III in 2) and eight healthy normal volunteers. Patients with diabetes mellitus were excluded. A dynamic PET study was performed for 40 min following the injection of 370 MBq of FDG after 50-g glucose loading. On the basis of a three-compartment model, MGU,  $K_1$ ,  $k_2$ , and  $k_3$  were computed on a pixel by pixel basis to generate LV myocardial parametric maps. FDG standardized uptake value (SUV) was also calculated using static images obtained 40 min after FDG injection. These metabolic values were compared with myocardial flow distribution (%Flow), LVEF, LV volumes, and LV wall thickening (WT) determined by gated myocardial single-photon emission computed tomography using QGS software in eight myocardial segments.

*Results:* MGU correlated positively with LV volumes and negatively with LVEF.  $K_1$  was significantly higher in the segments of the patients than in those of the normal volunteers ( $0.082 \pm 0.055$  vs  $0.041 \pm 0.017$  ml min<sup>-1</sup> g<sup>-1</sup>,  $p < 0.05$ ), although there was no difference in MGU between the

groups. On the other hand, SUV,  $k_2$ , and  $k_3$  did not differ significantly between the groups. Among the patients, the  $K_1$  values were significantly higher in the areas with impaired WT (%WT < 17%) ( $0.109 \pm 0.063$  vs  $0.069 \pm 0.062$  ml min<sup>-1</sup> g<sup>-1</sup>,  $p < 0.05$ ) and in the areas with flow reduction (%Flow < 71%) ( $0.112 \pm 0.076$  vs  $0.071 \pm 0.046$  ml min<sup>-1</sup> g<sup>-1</sup>,  $p < 0.05$ ).

*Conclusion:* These results indicate that glucose utilization was preserved in the patients with LV dysfunction, mainly due to an increase in glucose transport, particularly in the regions with severely impaired LV function. Thus, the quantitative assessment of myocardial glucose utilization by FDG dynamic PET may provide useful information for assessing the regional myocardial metabolic status in patients with LV dysfunction.

**Keywords:** Positron emission tomography – Heart failure – Glucose metabolism – Glucose transporter –  $^{18}\text{F}$ -FDG

**Eur J Nucl Med Mol Imaging (2005) 32:806–812**

DOI 10.1007/s00259-004-1743-2

## Introduction

$^{18}\text{F}$ -fluorodeoxyglucose positron emission tomography (FDG PET) imaging has been used to assess myocardial viability in clinical settings [1–10]. Myocardial glucose utilization (MGU) is preserved in viable myocardium and it may be modulated by myocardial energetic status or ischemia [10–14]. It has been reported that MGU is enhanced by increased energetic stress, pressure overload, and myocardial ischemia [12, 13]. Cellular and molecular mechanisms have been proposed to explain the enhancement of glucose

Nagara Tamaki (✉)  
Department of Nuclear Medicine,  
Hokkaido University Graduate School of Medicine,  
Kita-15, Nishi-7, Kita-ku, Sapporo 060-8638, Japan  
e-mail: natamaki@med.hokudai.ac.jp  
Tel.: +81-11-7067155, Fax: +81-11-7067155

utilization. It is presumed that glucose transport into myocardial cells regulates the rate of glucose metabolism in the myocardium [10, 12, 13, 15–20]. The sarcolemmal expressions of glucose transporters (GLUTs), such as GLUT1 and GLUT4, have an important role in increasing glucose transport into myocardial cells [10, 13, 21].

MGU is assessed quantitatively using dynamic FDG PET [22–26]. The graphical plot method is widely used [27]. However, glucose metabolic rate derived from this method is calculated using the  $k$  complex regardless of the values of  $K_1$ ,  $k_2$ , and  $k_3$ . Quantitative measurement of the myocardial glucose metabolic rate using a three-compartment model has been proposed [23], but its clinical implications have not been completely evaluated. The entry of glucose and its analogue is mainly regulated by glucose transporters [10]. In three-compartment analysis,  $K_1$  may indicate a rate constant of glucose transport from blood to myocardial cells. Therefore, the  $K_1$  value may reflect GLUT expression, which mainly depends on the process of glucose transport into myocardial cells. Myocardium with left ventricular (LV) dysfunction may show increased GLUT expression due to increased myocardial energetic stress; therefore, the individual assessment of each  $k$  value may provide new information regarding myocardial pathological conditions in a clinical setting. The aim of this study was to evaluate whether  $K_1$ ,  $k_2$ , and  $k_3$  values are affected in myocardium with LV dysfunction.

## Materials and methods

### Study population

Ten patients with LV dysfunction (eight males and two females, mean age  $62 \pm 8$  years) were enrolled in this study. The clinical characteristics are shown in Table 1. The ten patients comprised seven with idiopathic dilated cardiomyopathy (DCM) and three with aortic regurgitation (AR). The LV diastolic dimension and the percent fractional shortening were  $64.1 \pm 8.0$  mm and  $17.8\% \pm 8.5\%$ , respectively, on echocardiography. Patients with diabetes mellitus were excluded from this study. Plasma glucose concentration under the fasting condition was  $92.6 \pm 5.0$  mg/dl, and the percentage of hemoglobin A1c (HbA1c) was  $5.3\% \pm 0.2\%$  (normal upper limit  $< 5.6\%$ ). Seven pa-

tients underwent myocardial perfusion single-photon emission computed tomography (SPECT). All medical treatments were continued before the scan. Two out of seven patients did not undergo ECG-gated SPECT owing to atrial fibrillation. All patients were proved to have no significant coronary arterial stenosis by coronary angiography. As the control group, eight normal volunteers (all males, mean age  $33 \pm 5$  years) without any abnormal ECG findings at rest were enrolled in this study. They had no history of cardiac disease, hypertension, hyperlipidemia, or diabetes mellitus. Their fasting glucose and HbA1c levels were  $90.4 \pm 5.0$  mg/dl and  $5.1\% \pm 0.2\%$ , respectively. Six of the normal volunteers underwent ECG-gated myocardial perfusion SPECT. The study was approved by the Ethics Committee of Hokkaido University Hospital. Written informed consent was obtained from all the patients and normal volunteers.

### $^{18}\text{F}$ -FDG PET and data processing

PET imaging was performed using a whole-body scanner (EXACT HR+; CTI/Siemens, Knoxville, TN, USA). After a minimum of 6 h fasting, a 50-g glucose solution was administered orally 30 min before FDG injection. A 2D data acquisition was used in this study. A transmission scan was performed using an external source of  $^{68}\text{Ga}$ . Using an infusion pump, 370 MBq of FDG in 6 ml solution was injected intravenously over 3 min. After starting the injection, a dynamic PET data acquisition was performed for 40 min: 20 s $\times$ 4, 40 s $\times$ 4, 60 s $\times$ 4, 180 s $\times$ 4 and 300 s $\times$ 4. A static image was also obtained from 40 to 50 min after FDG injection. The intrinsic resolution of the system was 4.5 mm full-width at half-maximum.

Input function was assessed from the time–activity curve drawn in the left atrium on dynamic PET images. Based on a three-compartment model, parametric maps were computed using a non-linear least squares fitting method pixel by pixel, with the correction of spillover from cardiac chambers to the myocardium [23] (Fig 1). The value of  $k_4$  was assumed to be zero. The LV myocardium was divided into eight segments. The eight regions of interest (ROIs) for each case were drawn manually on the basal anterior, apical anterior, basal septum, apical septum, basal inferior, apical inferior, basal lateral, and apical lateral wall. The values of  $K_1$ ,  $k_2$ , and  $k_3$  were calculated for each ROI. MGU was calculated using the formula shown below. A blood sample was collected at the time of FDG injection to measure plasma glucose level, which was used for MGU calculation.

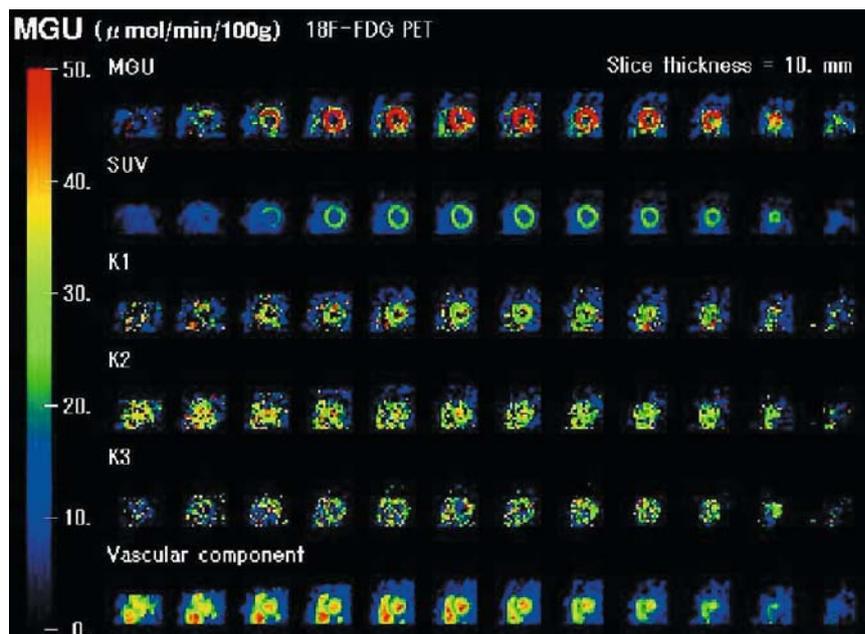
$$\text{MGU}(\mu\text{mol/g per min}) = 1/\text{LC} \times (K_1 \times k_3)/(k_2 + k_3) \times \text{Cp}$$

where LC is lumped constant ( $=0.67$ ) and Cp is the plasma glucose level (mmol/l). The standardized uptake value (SUV) of the

**Table 1.** Clinical characteristics of the ten patients

	Patient no.	Age (years)	Sex	Diagnosis	NYHA	%FS	LVDd (mm)	LAD (mm)	SPECT	QGS
	1	45	F	DCM	II	9	64	52		
	2	57	M	DCM	II	13	78	53		
	3	56	M	AR	II	24	59	48		N.D.
	4	69	M	DCM	III	23	60	41		
	5	64	F	DCM	II	16	61	40		
%FS percent fractional shortening, LVDd left ventricular dimension in the diastolic phase, LAD left atrial dimension, N.D. not done	6	65	M	DCM	II	7	54	35		
	7	69	M	DCM	III	20	62	75		N.D.
	8	57	M	DCM	II	8	78	51	N.D.	N.D.
	9	71	M	AR	II	27	66	43	N.D.	N.D.
	10	53	M	AR	II	31	59	49	N.D.	N.D.

**Fig. 1.** Typical parametric images of glucose metabolic parameters in a patient with DCM (case 1). Parametric maps of MGU, SUV,  $K_1$ ,  $k_2$ ,  $k_3$ , and vascular compartment are shown from the top row to the bottom row



myocardium was also calculated using a static image obtained 40–50 min after FDG injection and employing the formula:  $SUV = \text{myocardial uptake (Bq/g)} \times \text{body weight (g)} / \text{injected dose (Bq)}$ .

#### Myocardial perfusion SPECT

Myocardial perfusion SPECT was performed using a rotating dual-detector gamma camera with the detectors mounted at right angles and fitted with high-resolution collimators (Vertex; ADAC Laboratories, Milpitas, CA, USA). Data acquisition was started 30 min after the injection of 740 MBq  $^{99m}\text{Tc}$ -tetrofosmin at rest. The image acquisition variables included the following: a 140-keV photopeak with a 20% window, 64 projections at 40 s/projection over a  $180^\circ$  ( $90^\circ/\text{detector}$ ) elliptical orbit, a 38-cm roving detector mask, and a matrix size of  $64 \times 64$ . Acquisitions were gated for eight frames in a cardiac cycle.

The eight-interval projection data sets were prefiltered with a 2D Butterworth filter (order 2.5, critical frequency 0.22 cycles/pixel, pixel size 0.64 cm) and reconstructed with filtered backprojection using a ramp filter; no attenuation correction was performed. The resliced transaxial image sets were reoriented into short-axis sets that were then processed in the batch mode using a stand-alone workstation running automatic LVEF quantification software. The projection data sets were also summed and prefiltered with a 2D Butterworth filter (order 2.5, critical frequency 0.33 cycles/pixel, pixel size 0.64 cm), producing high-count short, vertical, and horizontal long-axis images for qualitative interpretation and for polar plot and circumferential count displays.

The LV myocardium was automatically divided into 20 segments according to quantitative perfusion SPECT (QPS) software (AutoQUANT; ADAC Lab., CA, USA). The most basal six segments and two apical regions were excluded from analysis. The average values of two regions in the septal and lateral segments corresponding to the segments on the FDG scan were calculated. A total of eight segments, comprising four basal and four apical segments, were used for analysis. The percentages of myocardial flow

(%Flow) of these eight segments were calculated using the values of QPS software.

Regional LV function was assessed on the basis of the wall thickening (WT), derived from QGS software [28], of the eight segments. LV global functional parameters, such as LVEF, end-diastolic volume (EDV) and end-systolic volume (ESV), were also calculated using QGS software. Additionally, the average value of eight segmental regional WT was used as an index of LV global function.

#### Data analysis

The values of the parameters were compared between the patients with LV dysfunction and the normal volunteers. In addition, among the patients, the values of glucose metabolic parameters were compared between the groups with and without perfusion or wall thickening abnormality. Perfusion and wall motion abnormalities were defined as less than 71% for %Flow, and less than 17% for WT, respectively. These cut-off values were obtained from the average values in patients, because values of normal volunteers were not obtained in this study.

#### Statistical analyses

The values are expressed as mean  $\pm$  SD. The differences in values were evaluated using a two-tailed unpaired *t* test. Regression analysis was performed using a linear regression method. A *p* value less than 0.05 was considered statistically significant.

## Results

The blood glucose level at the time of  $^{18}\text{F}$ -FDG injection was  $160 \pm 21$  mg/dl in the normal volunteers and  $131 \pm 29$  mg/dl in the patients ( $p=0.063$ ). There was no significant

**Table 2.** Comparison of parameters between normal volunteers and patients with LV dysfunction

	Normal volunteers	Patients	<i>p</i> value
MGU ( $\mu\text{mol}/100\text{ g per min}$ )	27.6 $\pm$ 12.7	35.8 $\pm$ 17.6	0.3290
SUV	4.07 $\pm$ 1.15	5.09 $\pm$ 1.75	0.1931
$K_1$ ( $\text{ml min}^{-1}\text{ g}^{-1}$ )	0.041 $\pm$ 0.017	0.082 $\pm$ 0.055	0.0170*
$k_2$ (/min)	0.071 $\pm$ 0.027	0.140 $\pm$ 0.122	0.1585
$k_3$ (/min)	0.100 $\pm$ 0.055	0.123 $\pm$ 0.088	0.7449
WT (%)	44.7 $\pm$ 6.1	17.0 $\pm$ 6.8	0.0058*
%Flow (%)	76.6 $\pm$ 4.5	71.7 $\pm$ 11.2	0.7182
EDV (ml)	93.6 $\pm$ 10.5	179.4 $\pm$ 5.0	0.0034*
ESV (ml)	40.6 $\pm$ 8.5	137.3 $\pm$ 54.0	0.0045*
EF (%)	56.8 $\pm$ 6.1	25.8 $\pm$ 5.0	<0.0001*

\**p*<0.05

difference in rate–pressure products between the patients and normal volunteers.

MGU did not differ between the two groups, but  $K_1$  in the patients with LV dysfunction was significantly higher than that in the normal volunteers (0.082 $\pm$ 0.055 vs 0.041 $\pm$ 0.017  $\text{ml min}^{-1}\text{ g}^{-1}$ , *p*<0.05) (Table 2). There was no significant difference in  $k_2$ ,  $k_3$  or SUV between the two groups.

Correlations between LV functional parameters and myocardial glucose metabolic parameters in patients are shown in Table 3. There were trends towards positive correlations between MGU and LV volumes, and an inverse correlation between MGU and EF. Moreover, MGU was inversely correlated with WT (*r*=−0.908, *p*<0.05).

In segment-based analysis, MGU,  $K_1$ , and SUV in the patients were significantly higher than those in normal volunteers (Table 2). However, there were no significant differences in  $k_2$  or  $k_3$  between the groups.

A comparison between patients with and patients without myocardial flow reduction is shown in Table 4. The  $K_1$  value in the segments with a flow reduction was significantly higher than the value in those without a flow reduction despite the absence of a difference in MGU (0.112 $\pm$ 0.076 vs 0.071 $\pm$ 0.046  $\mu\text{mol}/100\text{ g per min}$ , *p*<0.05).

**Table 3.** Correlation coefficient values between metabolic parameters and LV function

	EDV (ml)	ESV (ml)	EF (%)	WT (%)
MGU ( $\mu\text{mol}/100\text{ g per min}$ )	0.478	0.513	−0.551	−0.908*
SUV	0.264	0.216	0.290	0.333
$K_1$ ( $\text{ml min}^{-1}\text{ g}^{-1}$ )	0.031	0.056	−0.345	−0.864
$k_2$ (/min)	0.538	0.486	0.073	−0.352
$k_3$ (/min)	0.701	0.612	0.385	0.423

\**p*<0.05

**Table 4.** Comparison of parameters in segments with or without a flow reduction

	Segments with %Flow>71% (n=26)	Segments with %Flow<71% (n=14)	<i>p</i> value
MGU ( $\mu\text{mol}/100\text{ g per min}$ )	30.6 $\pm$ 16.7	36.3 $\pm$ 18.5	0.2470
SUV	4.63 $\pm$ 1.53	4.83 $\pm$ 1.62	0.5129
$K_1$ ( $\text{ml min}^{-1}\text{ g}^{-1}$ )	0.071 $\pm$ 0.046	0.112 $\pm$ 0.076	0.0407*
$k_2$ (/min)	0.134 $\pm$ 0.164	0.232 $\pm$ 0.244	0.0682
$k_3$ (/min)	0.156 $\pm$ 0.158	0.118 $\pm$ 0.099	0.7120
WT (%)	18.2 $\pm$ 5.1	12.3 $\pm$ 7.1	0.0034*
%Flow	79.1 $\pm$ 5.7	59.4 $\pm$ 9.2	<0.0001*

\**p*<0.05

**Table 5.** Comparison of parameters in segments with or without impaired WT

	Segments with WT>17% (n=30)	Segments with WT<17% (n=10)	<i>p</i> value
MGU ( $\mu\text{mol}/100\text{ g per min}$ )	34.0 $\pm$ 18.2	42.9 $\pm$ 19.0	0.1403
SUV	5.18 $\pm$ 1.76	4.68 $\pm$ 1.35	0.6197
$K_1$ ( $\text{ml min}^{-1}\text{ g}^{-1}$ )	0.069 $\pm$ 0.062	0.109 $\pm$ 0.063	0.0193*
$k_2$ (/min)	0.105 $\pm$ 0.112	0.197 $\pm$ 0.220	0.0208*
$k_3$ (/min)	0.203 $\pm$ 0.168	0.110 $\pm$ 0.098	0.1328
WT (%)	19.5 $\pm$ 3.7	8.2 $\pm$ 4.4	<0.0001*
%Flow (%)	75.7 $\pm$ 9.8	66.1 $\pm$ 12.1	0.0047*

\**p*<0.05

Furthermore, the segments with impaired WT had a higher  $K_1$  value than those without impaired WT (Table 5, 0.109 $\pm$ 0.063 vs 0.069 $\pm$ 0.062, *p*<0.05).

## Discussion

The major finding of this study is preserved MGU in patients with LV dysfunction, mainly due to an increased  $K_1$  value. The increase in  $K_1$  was most significant in the myocardial segments with perfusion and wall thickening abnormalities despite the absence of a difference in MGU. This analysis method provides values of each of the glucose metabolic parameters, including  $K_1$ ,  $k_2$ , and  $k_3$ . These parameters seem to be useful in understanding the pathophysiological status of patients with LV dysfunction. Altered glucose transporters and glucose metabolism may be associated with the severity of the disease.

### *Comparison of glucose metabolism and GLUT expression*

In experimental model studies, myocardial GLUT distribution and expression are affected by various stresses, such as ischemia, hypoxia, or left ventricular volume overload [10, 12, 15, 20, 29, 30]. On the other hand, Paternostro et al. reported that explanted failing human heart showed an increased GLUT-1 expression level and a decreased GLUT-4/GLUT-1 ratio [17]. Therefore, enhanced glucose utilization in patients with LV dysfunction may be due to an increased GLUT expression or translocation of GLUT in the myocardial cells. In this study, enhanced MGU in patients with LV dysfunction may be induced by increased myocardial wall stress or ischemia via enhanced GLUT expression or GLUT translocation. A significant increase in the  $K_1$  value in patients may indicate increased GLUT distribution on the surface of myocardial cells. Enhanced or preserved myocardial glucose utilization is presumed to be beneficial for a heart which is under ischemia, or under increased pressure or volume overload [19, 31–33]. Metabolic switching from fatty acid to glucose metabolism via a molecular mechanism may be an adaptive response against ischemia or energetic stress [19]. On the other hand, recent data suggest that there is no difference in GLUT-1 and GLUT-4 expression in patients with non-ischemic heart failure in comparison with patients who have a non-failing heart. Thus, the biological relevance of an increased  $K_1$  value is controversial [34]. Rate constant values derived using the three-compartment model may provide additional information regarding the myocardial glucose metabolic status and also GLUT activity in the myocardium, which may be useful to understand cardiac pathophysiology in a clinical setting. Moreover, it may be useful to provide new approaches to treat patients with coronary artery disease or a failing heart [10, 12, 19].

### *Comparison with ventricular dysfunction*

An increase in MGU with an enhanced  $K_1$  in patients with LV dysfunction may indicate that the myocardium with abnormal function preserves glucose utilization by enhancing  $K_1$ , which would seem to be a compensational effect. This finding is compatible with enhanced glucose utilization for hearts under increased stress or ischemia [12]. Furthermore, an increased  $K_1$  value may reflect an increased GLUT expression level on the myocardial cell surface [29–31]. This may be a cardiac protective function [10, 13]. In the present study, MGU positively correlated with LV volume and negatively correlated with WT, indicating the relationship between myocardial glucose utilization and global LV function. Severe LV functional abnormality may induce enhanced glucose utilization. On the other hand, preserved glucose utilization in these segments may indicate the absence of significant fibrotic changes in our limited number of patients. A further study of a large number of patients is required to confirm our preliminary findings.

There was no significant difference in  $k_2$  and  $k_3$  values between the patients and the normal volunteers. There was

also wide variability in the values of  $k_2$  and  $k_3$ , particularly in the patients. This wide variability may reflect some aspects of glucose metabolic abnormality. However, the variability did not differ between the causes of LV dysfunction in this study.

### *Comparison with perfusion and wall thickening abnormalities*

In this comparative study of patients with and patients without myocardial flow reduction and WT abnormality, there was a significant increase in  $K_1$  values in the segments with flow reduction and WT reduction compared with the segments without such findings. However, MGU was not significantly different between the two groups. These findings may indicate that  $K_1$  is a more sensitive index than MGU for the assessment of regional abnormality or disease severity. Although the precise mechanism underlying these findings is uncertain, an increased  $k_2$  value may indicate increased efflux of glucose from myocardium to blood or impaired phosphorylation activity, which may be represented as the value of  $k_3$ . In this study, the  $k_3$  value in segments with a severe WT abnormality tended to be lower than in those without such an abnormality. Myocardial WT may be closely associated with the metabolic status of the myocardium rather than with myocardial perfusion. In the quantitative analysis of glucose metabolism and the turnover rate of the tracer, partial volume effect should be considered. MGU may be greatly influenced by the partial volume effect, whereas the turnover rate of the tracer may be less affected. Therefore,  $K_1$  may be more sensitive in assessing the alteration in glucose metabolism than MGU, particularly in the dysfunctional segments. An increased  $K_1$  value may also be due to technical failure when fitting the time–activity curves of the blood pool and myocardium in the thinned myocardium for the appropriate mathematical model. In this respect, a basic study may be warranted to determine the technical reliability of each value under various conditions.

### *Advantages of compartment analysis in comparison with SUV measurements*

SUV is considered a simple index for quantification of FDG uptake in the ROIs, and this technique has been used for the quantitative analysis of myocardial glucose utilization [35]. However, SUV may have a limitation in assessing the precise myocardial glucose metabolic status. In the assessment of cerebral glucose utilization, SUV exhibited limited accuracy in quantifying cerebral glucose metabolic status when compared with that derived using compartment analysis [36]. In myocardial analysis, too, myocardial metabolic conditions vary due to metabolic or myocardial pathological conditions. In particular, three-compartment analysis permits independent quantitative estimates of the rate constants  $K_1$ ,  $k_2$ , and  $k_3$  as well as the glucose metabolic rate. Considering these observations, compartment analysis may

provide insights into the precise myocardial pathophysiological status.

### Study limitations

One of the major limitations of this study is the limited number of patients investigated. There seems to have been relatively large fluctuation in the estimated values due to pixel by pixel calculation. A further study with more patients might minimize such variation and yield more confident findings.

In this study,  $^{18}\text{F}$ -FDG PET was performed after oral glucose loading, which may not maximize glucose utilization compared with hyperinsulinemic euglycemic clamp. In addition, the oral glucose loading technique may not ensure maintenance of the steady state condition for measurement of the kinetic constants or MGU. It has been reported that there is no difference in assessment of MGU between insulin clamp and oral glucose loading. However, the  $k$  complex value was lower in glucose loading than that in insulin clamp [37]. An increased  $K_1$  value in patients with LV dysfunction was shown in this study after oral glucose loading. Moreover, the plasma glucose level of normal volunteers at the time of  $^{18}\text{F}$ -FDG injection tended to be higher than that of patients with LV dysfunction, which likely explains that absence of a difference in MGU between the groups. Therefore, this increased  $K_1$  value in patients seems to be a significant finding. However, measurement of glucose metabolic parameters under the steady state during hyperinsulinemic euglycemic clamp is needed to assess precise glucose metabolic parameters.

Patients with diabetes mellitus were excluded from this study, but there is a possibility of glucose tolerance abnormality in the participating patients. Consequently, the insulin level after glucose loading may be lower than that in patients without glucose tolerance abnormality. Initial glucose transport via GLUT-4 depends on the insulin level [10, 13, 16]. In addition, an insulin-induced GLUT-1 translocation pathway has been shown in a rat heart model [38]. Therefore, the  $K_1$  value is assumed to be low in patients with glucose intolerance. In this study, the  $K_1$  value was increased in patients, particularly in segments with impaired wall thickening. These findings indicate that increased MGU and  $K_1$  values may be true in patients with LV dysfunction, even though the patients may have glucose intolerance. Substrates such as fatty acid and lactate may alter myocardial glucose transport, but they were not measured in this study.

Myocardial perfusion was assessed using SPECT without using PET. Percent flow (%Flow) represents relative flow distribution. Absolute myocardial blood flow measurement makes it possible to evaluate the precise relationship between myocardial blood flow and glucose metabolic status. However, the patients in this study did not have ischemic heart disease. Myocardial perfusion abnormality was mainly used to assess myocardial damage such as fibrotic changes. Additionally,  $K_1$  may be dependent upon the level of myocardial perfusion, but it was not quantified

in this study. A precise comparative study between glucose metabolic parameters and myocardial blood flow is needed.

In computing the parametric map of glucose metabolic parameters, spillover from blood activity into myocardial tissue was corrected [23]. However, accurate correction seems to be difficult. An insufficient spillover correction may cause overestimation of the  $K_1$  value. This problem may be solved by means of phantom or blood pool imaging using  $^{11}\text{C}$ -labeled carbon monoxide. Additionally, partial volume effect was not corrected in this study, because there was no significant difference in LV wall thickness between patients and normal volunteers.

Lumped constant (LC) was used as a constant with a value of 0.67. It has been reported that LC is not a constant and that the value for deoxyglucose decreases when myocardial glucose uptake is enhanced [39]. In this study, the myocardium in the patients may have had a low LC, so there is a possibility that the calculated MGU may have been underestimated.

### Conclusion

Preserved glucose utilization mainly due to an increase in the  $K_1$  value was demonstrated in patients with LV dysfunction. This finding was significant in the myocardial segments with severely impaired LV function. Therefore, quantitative assessment of myocardial glucose utilization by FDG dynamic PET and three-compartment analysis may provide useful information on the regional myocardial metabolic status in patients with LV dysfunction.

### References

1. Marshall RC, Tillisch JH, Phelps ME, Huang SC, Carson R, Henze E, et al. Identification and differentiation of resting myocardial ischemia and infarction in man with positron computed tomography,  $^{18}\text{F}$ -labeled fluorodeoxyglucose and N-13 ammonia. *Circulation* 1983;67:766–78.
2. Tillisch J, Brunken R, Marshall R, Schwaiger M, Mandelkern M, Phelps M, et al. Reversibility of cardiac wall-motion abnormalities predicted by positron tomography. *N Engl J Med* 1986; 314:884–8.
3. Schwaiger M, Brunken R, Grover-McKay M, Krivokapich J, Child J, Tillisch JH, et al. Regional myocardial metabolism in patients with acute myocardial infarction assessed by positron emission tomography. *J Am Coll Cardiol* 1986;8:800–8.
4. Brunken R, Schwaiger M, Grover-McKay M, Phelps ME, Tillisch J, Schelbert HR. Positron emission tomography detects tissue metabolic activity in myocardial segments with persistent thallium perfusion defects. *J Am Coll Cardiol* 1987;10:557–67.
5. Tamaki N, Yonekura Y, Yamashita K, Senda M, Saji H, Hashimoto T, et al. Relation of left ventricular perfusion and wall motion with metabolic activity in persistent defects on thallium-201 tomography in healed myocardial infarction. *Am J Cardiol* 1988;62:202–8.
6. Camici P, Ferrannini E, Opie LH. Myocardial metabolism in ischemic heart disease: basic principles and application to imaging by positron emission tomography. *Prog Cardiovasc Dis* 1989;32:217–38.

7. Bonow RO, Dilsizian V, Cuocolo A, Bacharach SL. Identification of viable myocardium in patients with chronic coronary artery disease and left ventricular dysfunction. Comparison of thallium scintigraphy with reinjection and PET imaging with <sup>18</sup>F-fluoro-deoxyglucose. *Circulation* 1991;83:26–37.
8. Tamaki N, Kawamoto M, Tadamura E, Magata Y, Yonekura Y, Nohara R, et al. Prediction of reversible ischemia after revascularization. Perfusion and metabolic studies with positron emission tomography. *Circulation* 1995;91:1697–1705.
9. Depre C, Vanoverschelde JL, Gerber B, Borgers M, Melin JA, Dion R. Correlation of functional recovery with myocardial blood flow, glucose uptake, and morphologic features in patients with chronic left ventricular ischemic dysfunction undergoing coronary artery bypass grafting. *J Thorac Cardiovasc Surg* 1997;113:371–78.
10. Depre C, Vanoverschelde JL, Taegtmeyer H. Glucose for the heart. *Circulation* 1999;99:578–88.
11. McFalls EO, Baldwin D, Palmer B, Marx D, Jaimes D, Ward HB. Regional glucose uptake within hypoperfused swine myocardium as measured by positron emission tomography. *Am J Physiol* 1997;272:H343–9.
12. Young LH, Russell RR 3rd, Yin R, Caplan MJ, Ren J, Bergeron R, et al. Regulation of myocardial glucose uptake and transport during ischemia and energetic stress. *Am J Cardiol* 1999;83:25H–30H.
13. Young LH, Coven DL, Russell RR 3rd. Cellular and molecular regulation of cardiac glucose transport. *J Nucl Cardiol* 2000;7:267–76.
14. McFalls EO, Murad B, Liow JS, Gannon MC, Haspel HC, Lange A, et al. Glucose uptake and glycogen levels are increased in pig heart after repetitive ischemia. *Am J Physiol Heart Circ Physiol* 2002;282:H205–11.
15. Brosius FC 3rd, Liu Y, Nguyen N, Sun D, Bartlett J, Schwaiger M. Persistent myocardial ischemia increases GLUT1 glucose transporter expression in both ischemic and non-ischemic heart regions. *J Mol Cell Cardiol* 1997;29:1675–85.
16. Zorzano A, Sevilla L, Camps M, Becker C, Meyer J, Kammermeier H, et al. Regulation of glucose transport, and glucose transporter expression and trafficking in the heart: studies in cardiac myocytes. *Am J Cardiol* 1997;80:65A–76A.
17. Paternostro G, Pagano D, Gneccchi-Ruscione T, Bonser RS, Camici PG. Insulin resistance in patients with cardiac hypertrophy. *Cardiovasc Res* 1999;42:246–53.
18. Southworth R, Dearling JL, Medina RA, Flynn AA, Pedley RB, Garlick PB. Dissociation of glucose tracer uptake and glucose transporter distribution in the regionally ischaemic isolated rat heart: application of a new autoradiographic technique. *Eur J Nucl Med Mol Imaging* 2002;29:1334–41.
19. Taegtmeyer H. Switching metabolic genes to build a better heart. *Circulation* 2002;106:2043–5.
20. McFalls EO, Murad B, Haspel HC, Marx D, Sikora J, Ward HB. Myocardial glucose uptake after dobutamine stress in chronic hibernating swine myocardium. *J Nucl Cardiol* 2003;10:385–94.
21. Russell RR, 3rd, Bergeron R, Shulman GI, Young LH. Translocation of myocardial GLUT-4 and increased glucose uptake through activation of AMPK by AICAR. *Am J Physiol* 1999;277:H643–9.
22. Ratib O, Phelps ME, Huang SC, Henze E, Selin CE, Schelbert HR. Positron tomography with deoxyglucose for estimating local myocardial glucose metabolism. *J Nucl Med* 1982;23:577–86.
23. Gambhir SS, Schwaiger M, Huang SC, Krivokapich J, Schelbert HR, Nienaber CA, et al. Simple noninvasive quantification method for measuring myocardial glucose utilization in humans employing positron emission tomography and fluorine-18 deoxyglucose. *J Nucl Med* 1989;30:359–66.
24. Choi Y, Hawkins RA, Huang SC, Gambhir SS, Brunken RC, Phelps ME, et al. Parametric images of myocardial metabolic rate of glucose generated from dynamic cardiac PET and 2-[<sup>18</sup>F] fluoro-2-deoxy-D-glucose studies. *J Nucl Med* 1991;32:733–8.
25. Hicks RJ, Herman WH, Kalf V, Molina E, Wolfe ER, Hutchins G, et al. Quantitative evaluation of regional substrate metabolism in the human heart by positron emission tomography. *J Am Coll Cardiol* 1991;18:101–11.
26. Marinho NV, Keogh BE, Costa DC, Lammerstma AA, Ell PJ, Camici PG. Pathophysiology of chronic left ventricular dysfunction. New insights from the measurement of absolute myocardial blood flow and glucose utilization. *Circulation* 1996;93:737–44.
27. Patlak CS, Blasberg RG. Graphical evaluation of blood-to-brain transfer constants from multiple-time uptake data. Generalizations. *J Cereb Blood Flow Metab* 1985;5:584–90.
28. Germano G, Erel J, Lewin H, Kavanagh PB, Berman DS. Automatic quantitation of regional myocardial wall motion and thickening from gated technetium-99 m sestamibi myocardial perfusion single-photon emission computed tomography. *J Am Coll Cardiol* 1997;30:1360–7.
29. Sun D, Nguyen N, DeGrado TR, Schwaiger M, Brosius FC 3rd. Ischemia induces translocation of the insulin-responsive glucose transporter GLUT4 to the plasma membrane of cardiac myocytes. *Circulation* 1994;89:793–8.
30. Young LH, Renfu Y, Russell R, Hu X, Caplan M, Ren J, et al. Low-flow ischemia leads to translocation of canine heart GLUT-4 and GLUT-1 glucose transporters to the sarcolemma in vivo. *Circulation* 1997;95:415–22.
31. Brosius FC 3rd, Nguyen N, Egert S, Lin Z, Deeb GM, Haas F, et al. Increased sarcolemmal glucose transporter abundance in myocardial ischemia. *Am J Cardiol* 1997;80:77A–84A.
32. Abel ED, Kaulbach HC, Tian R, Hopkins JC, Duffy J, Doetschman T, et al. Cardiac hypertrophy with preserved contractile function after selective deletion of GLUT4 from the heart. *J Clin Invest* 1999;104:1703–14.
33. Liao R, Jain M, Cui L, Dâ Agostino J, Aiello F, Luptak I, et al. Cardiac-specific overexpression of GLUT1 prevents the development of heart failure attributable to pressure overload in mice. *Circulation* 2002;106:2125–31.
34. Razeghi P, Young ME, Cockrill TC, Frazier OH, Taegtmeyer H. Downregulation of myocardial myocyte enhancer factor 2C and myocyte enhancer factor 2C-regulated gene expression in diabetic patients with nonischemic heart failure. *Circulation* 2002;106:407–11.
35. Tamaki N, Yonekura Y, Kawamoto M, Magata Y, Sasayama S, Takahashi N, et al. Simple quantification of regional myocardial uptake of fluorine-18-deoxyglucose in the fasting condition. *J Nucl Med* 1991;32:2152–7.
36. Yamaji S, Ishii K, Sasaki M, Mori T, Kitagaki H, Sakamoto S, et al. Evaluation of standardized uptake value to assess cerebral glucose metabolism. *Clin Nucl Med* 2000;25:11–6.
37. Knuuti MJ, Nuutila P, Ruotsalainen U, Saraste M, Harkonen R, Ahonen A, et al. Euglycemic hyperinsulinemic clamp and oral glucose load in stimulating myocardial glucose utilization during positron emission tomography. *J Nucl Med* 1992;33:1255–62.
38. Egert S, Nguyen N, Schwaiger M. Myocardial glucose transporter GLUT1: translocation induced by insulin and ischemia. *J Mol Cell Cardiol* 1999;31:1337–44.
39. Hashimoto K, Nishimura T, Imahashi KI, Yamaguchi H, Hori M, Kusuoka H. Lumped constant for deoxyglucose is decreased when myocardial glucose uptake is enhanced. *Am J Physiol* 1999;276:H129–33.